persists at detectable concentrations in the nuclei of daughter cells. To examine this possibility, we performed similar experiments but applied BrdU about 12 hours later at stages 17 to 18, during the peak of motor neuron generation (*14*). Again, few (<1%) Islet-1–positive cells had incorporated BrdU within 4 hours (Table 2). If the cells that had begun to express Islet-1 at stages 15 to 16 underwent further rounds of cell division, then this should have been reflected by the rapid (<4 hours) incorporation of BrdU into Islet-1–positive cells at stages 17 to 18, which was not observed (Table 2). These results reinforce the conclusion that Islet-1 is expressed only in postmitotic motor neurons. The small percentage of cells that coexpress Islet-1 and BrdU within 4 hours may reflect cells that are labeled at late stages of S phase.

24. Notochords from stage 10 and floor plate tissue from stages 17 to 18 chick embryos were grafted adjacent to the caudal neural tube of stage 10 hosts (*4*). Approximately 48 hours after grafting, the embryos were fixed and serial sections were stained with antibodies to Islet-1, SC1, and FP1.
25. A segment of notochord was removed from the caudal region of the neural tube of stage 9 to 10 chick embryos [M. Placzek, M. Tessier-Lavigne, T. Yamada, T. Jessell, J. Dodd, *Science* **250**, 985 (1990); also (*4*)]. Approximately 48 hours after removal of the notochord, the embryos were fixed and serial sections stained with antibodies to Islet-1, SC1, CRABP, AC4, and FP1 (*4, 5*).
26. J. S. Eisen, *Science* **252**, 569 (1991).
27. W. McGinnis and R. Krumlauf, *Cell* **68**, 283 (1992).
28. D. Duboule and P. Dolle, *EMBO J.* **8**, 1497 (1989); A. Graham, N. Papalopulu, R. Krumlauf, *Cell* **57**, 367 (1989); P. Hunt *et al.*, *Nature* **353**, 861 (1991).
29. M. D. Goulding *et al.*, *EMBO J.* **10**, 1135 (1991); C. Walther and P. Gruss, *Development* **113**, 1435 (1991).
30. O. Chisaka and M. R. Capecchi, *Nature* **350**, 473 (1991); T. Lufkin, A. Dierich, M. Lemeur, M. Mark, P. Chambon, *Cell* **66**, 1105 (1991); D. J. Epstein, M. Vekemons, P. Gros, *ibid.* **67**, 767 (1991); C. C. Ton *et al.*, *ibid.*, p. 1059; R. E. Hill *et al.*, *Nature* **354**, 522 (1991).
31. We thank J. Dodd, A. Furley, M. Placzek, and A. Ruiz i Altaba for comments on the manuscript and V. Leon for secretarial assistance. We also thank E. Carpenter for communicating results before publication and L. Role for discussion. This work was supported, in part, by grants from the Swedish National Science Research Council, Swedish Medical Research Council, Swedish National Board for Technical Development, and the Juvenile Diabetes Foundation, New York, to T.E. T.Y. is an associate and T.M.J. is an investigator of the Howard Hughes Medical Institute.

4 February 1992; accepted 14 April 1992

Galactose Oxidation in the Design of Immunogenic Vaccines

Biao Zheng, Sara J. Brett, John P. Tite, M. Robert Lifely, Thomas A. Brodie, John Rhodes*

Potent immunological adjuvants are urgently required to complement recombinant and synthetic vaccines. However, it has not been possible to derive new principles for the design of vaccine adjuvants from knowledge of the mechanism of immunogenicity. Carbonyl-amino condensations, which are essential to the inductive interaction between antigen-presenting cells and T helper cells, were tested as a target for the enhancement of immune responses. Enzymic oxidation of cell-surface galactose to increase amine-reactive carbonyl groups on murine lymphocytes and antigen–presenting cells provided a potent, noninflammatory method of enhancing the immunogenicity of viral, bacterial, and protozoal subunit vaccines in mice.

Vaccination, the most effective means of combatting infectious disease, requires the use of adjuvants that nonspecifically enhance the immunogenicity of attenuated, killed, or fragmented microorganisms. This is particularly important for recombinant proteins and synthetic peptides, which are substantially less immunogenic than conventional vaccines. Aluminum salts (alum), first described as adjuvants more than 60 years ago (*1*), remain the only agents approved for human use. Their potency is limited and they do not consistently enhance cell-mediated responses likely to be important in antiviral immunity. New vaccine adjuvants and vehicles at the preclinical research stage include surface-active agents, liposomes, immune-stimulating complexes (ISCOMS), and adjuvant peptides (*2*). These approaches seek to mimic general properties of infectious pathogens such as persistence, size, lipophilicity, and the ability to stimulate macrophages nonspecifically. Alternatively, live attenuated vectors have been developed that, because of their ability to productively infect a susceptible host, confer immunogenicity on the recombinant antigens they carry (*3*). In contrast to these approaches, we have targeted covalent chemical events between cellular ligands that appear to be essential to immune induction.

The primary specific event in most immune responses is the inductive interaction between antigen (Ag)–presenting cells (APC) and T helper lymphocytes (T_H cells) (*4*). In addition to the recognition that takes place between the T cell receptor and the complex of Ag and major histocompatibility complex (MHC) class II molecule, essential accessory interactions occur at the macromolecular level (*5*). At the chemical level, transient carbonyl-amino condensation (Schiff base formation) between cell-surface ligands also appears to be essential for Ag-specific T cell activation (*6*). This reaction might provide a means of enhancing responses to potential vaccines by increasing the expression of reactive ligands. To test this idea, we used galactose

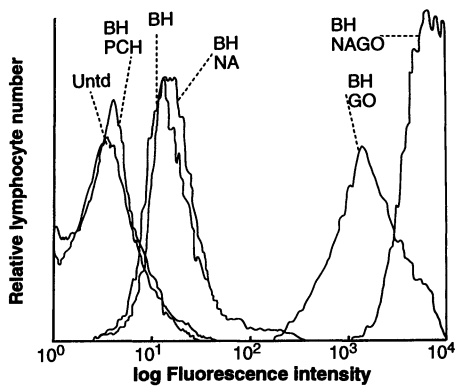

Fig. 1. Flow cytofluorometric measurement of amine-reactive carbonyl groups on the lymphocyte surface. Freshly prepared murine (BALB/c) spleen cells (5×10^6/ml in PBS) were treated with biotin hydrazide (Sigma, Poole, Dorset, United Kingdom) (5 mM, 1 hour, 37°C), which forms a covalent hydrazone (C = N) linkage with reactive carbonyl groups. This reversible bond was then reduced with $NaCNBH_3$ at neutral pH (10 mM, 1 hour, 20°C). After the reduction, cells were washed, treated with fluorescein isothyocyanate (FITC)–avidin (Vector Laboratories, Peterborough, United Kingdom) (1:50 dilution) (for 30 min at 4°C), and washed three times. Flow cytofluorometric measurements (gated on lymphocytes) were obtained with a FACScan (Becton Dickinson), with the use of Consort 30 data management. Pyridinium chloride hydrazide (Sigma) treatment was at 10 mM for 1 hour at 37°C, followed by reduction with $NaCNBH_3$. Cells were exposed to neuraminidase at 2.5 U/ml for 30 min at 37°C and washed. Treatment with GO (5 U/ml) and with NAGO (NA 2.5 U/ml; GO 5 U/ml) was performed in the same way. Lymphocytes were exposed to the following: FITC-avidin only (Untd); pyridinium chloride hydrazide and then to biotin hydrazide (BH PCH); biotin hydrazide (BH); NA and then to biotin hydrazide (BH NA); GO and then to biotin hydrazide (BH GO); and NAGO and then to biotin hydrazide (BH NAGO).

B. Zheng and J. Rhodes, Department of Pharmacology, Wellcome Research Laboratories, Langley Court, South Eden Park Road, Beckenham, Kent, United Kingdom BR3 3BS.
S. J. Brett, J. P. Tite, M. R. Lifely, Department of Cell Biology, Wellcome Research Laboratories, Beckenham, Kent, United Kingdom BR3 3BS.
T. A. Brodie, Department of Drug Safety Evaluation, Wellcome Research Laboratories, Beckenham, Kent, United Kingdom BR3 3BS.

*To whom correspondence should be addressed.

oxidase (GO), which generates cell-surface aldehydes on C-6 of terminal D-galactosyl and *N*-acetyl-D-galactosaminyl residues (*7*). We optimized the process by adding neuraminidase (NA) to further expose cell-surface substrate. Constitutive amine-reactive carbonyl groups were observed at the surface of murine lymphocytes and were increased 100-fold after galactose oxidation (Fig. 1). NA had little effect on the availability of constitutive ligands but substantially increased the availability of substrate for GO (threefold). Although galactose oxidation has long been known to induce T cell proliferation in vitro (*7*), we had no reason to test its adjuvant potential until carbonyl-amino condensation had been implicated in the induction of immune responses.

Intravenous infusion of NAGO-modified APC produced substantial enhancement of specific T_H cell priming in vivo (ten times greater than with unmodified APC), but NAGO was even more effective when administered directly. To achieve potent adjuvant effects, we mixed small amounts of NAGO with Ag in aqueous solution and administered the mixture subcutaneously (*8*). In Fig. 2A, NAGO is compared with Freund's complete adjuvant (FCA) in the priming of regional lymph node T cells to the human immunodeficiency virus (HIV)-1_{IIIB} envelope subunit gp120 that had been derived from a baculovirus expression system [gp120(bac)] (*9*). Although FCA produced substantial priming, NAGO was markedly better, yielding a tenfold higher response to challenge with gp120(bac) and a fivefold higher response to challenge with gp120(CHO) [gp120-(CHO) is derived from Chinese hamster ovary (CHO) cells] (*9*). T cell priming to gp120(CHO) produced a similar result (Fig. 2B). One-twentieth the amount of gp120 was required to produce the same secondary response in vitro when NAGO replaced FCA in priming. Greater glycosylation occurs in the CHO-derived glycoprotein and, although possible modification of carbohydrates on Ag by NAGO is of interest, it is clearly not an obstacle to the adjuvant effect. In vitro secondary responses by lymph node cells (LNC) from NAGO-primed mice were completely inhibited by antibodies to CD4 or a combination of monoclonal antibodies to IA and IE (*10*). NAGO was also more effective than both FCA and alum in priming T cells to a short synthetic peptide corresponding to the immunodominant T_H cell epitope of influenza A nucleoprotein in B10S mice (*11*) (Fig. 2C).

Because NAGO is so effective in T cell priming, we tested whether it would induce unwanted reversal of genetically determined nonresponsiveness and thus potentially cause autoreactivity. Genetically determined nonresponsiveness was maintained in B10S mice given NAGO plus NP peptide 206-228, which is a BALB/c, but not a B10S, T_H cell determinant (*11*) (Fig. 2D). In contrast, NAGO produced a strong adjuvant effect with this peptide in the responder strain. NAGO proved to be a potent adjuvant in T cell priming to the P69 (pertactin) subunit of *Bordetella pertussis* (*12*) (expressed in *Pichia pastoralis*) and was comparable in effectiveness to FCA (Fig. 2E). In T cell priming to the precursor of the major malarial merozoite surface antigens (*13*) (recombinant baculovirus–derived PMMSA), NAGO was superior to both alum and saponin and comparable to FCA (Fig. 2F).

NAGO was effective as an adjuvant in the induction of secondary antibody responses to HIV-gp120(CHO), producing titers comparable to FCA and saponin, whereas alum was ineffective. Reciprocal $\log_{10}$ titers in groups of four CBA mice primed with 1 μg of protein subcutaneously and boosted with the same material 12

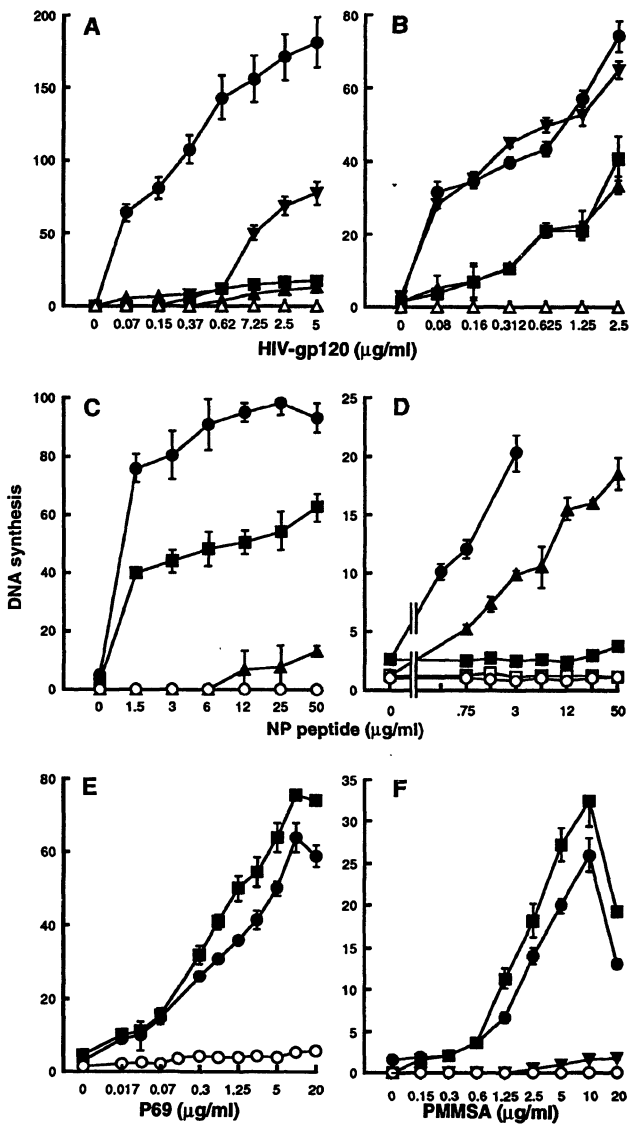

Fig. 2. T_H cell responses (^{3}H-TdR incorporation, cpm × 10^{-3} ± SE). (**A**) CBA/T6T6 mice received a single s.c. injection (1 μg) of HIV-gp120(bac) from the IIIB strain of HIV (American Biotechnologies, Inc., Cambridge, MA) with or without adjuvant. After 7 days regional (inguinal) LNC were prepared and restimulated (restim.) with gp120(bac) or gp120(CHO) in vitro. NAGO, gp120(bac) restim. (●); NAGO, gp120(CHO) restim. (▼); FCA, gp120(bac) restim. (■); FCA, gp120(CHO) restim. (▲); no adjuvant, gp120(bac) restim. (○); no adjuvant, gp120(CHO) restim. (△). (**B**) Mice received a single injection (1 μg) of HIV-gp120(CHO) (Celltech, Slough, United Kingdom). Priming was measured by restimulation as above. NAGO, gp120(CHO) restim. (●); NAGO, gp120(bac) restim. (▼); FCA, gp120(CHO) restim. (■); FCA, gp120(bac) restim. (▲); no adjuvant, gp120(CHO) restim. (○); no adjuvant, gp120(bac) restim. (△). (**C**) B10S mice received a single s.c. injection (5 μg) of NP peptide 260-283 with or without adjuvant. After 7 days LNC were restimulated with peptide in vitro. NAGO (●); FCA (■); alum (▲); no adjuvant (○). (**D**) Maintenance of genetically determined nonresponsiveness to influenza peptides. Mice received a single s.c. injection of peptide (20 μg) with or without NAGO as adjuvant. T_H cell priming in regional lymph nodes was measured after 7 days by restimulation. NP p206-228 (BALB/c epitope) with NAGO in BALB/c (●); NP p206-228 in B10S (□); NP p206-228 with NAGO in B10S (■); NP peptide 260-283 (B10S epitope) with NAGO in B10S (▲); no antigen (○). Proliferative responses are lower than in (C) because a higher than optimal dose of NAGO was used. (**E**) B10S mice received a single s.c. injection (1 μg) of the P69 subunit of *Bordetella pertussis* with or without adjuvant. Priming in regional lymph nodes was measured after 7 days by restimulation. NAGO (●); FCA (■); no adjuvant (○). (**F**) B10S mice received a single s.c. injection (2 μg) of the precursor to the major malarial merozoite surface antigens (rPMMSA) with or without adjuvant. Priming in regional lymph nodes was measured after 7 days. NAGO (●); FCA (■); saponin (▼); alum (△); no adjuvant (○). LNC proliferation assays were performed in microcultures with the use of Click's extra-high amino acid medium plus 0.5% normal mouse serum (*11*).

weeks later [FCA-primed mice received Freund's incomplete adjuvant (FIA)] were as follows: FCA, 4.4, 4.4, 4.4, 2.6; saponin, 4.4, 4.4, 4.4, 3.2; NAGO, 4.4, 3.8, 2.6, 2.6; alum, 2.3, <1.0, <1.0, <1.0. Serum was sampled 2 weeks after boosting. NAGO was also more effective than alum in priming for a secondary antibody response to the carbohydrate component of a *Neisseria meningitidis* group B (meningococcal meningitis) vaccine (*14*). The carbohydrate composition of the vaccine (which NAGO could in principle modify) was not an obstacle to the adjuvant effect. Mice (four per group) received a primary subcutaneous (s.c.) immunization with 100 μl of MB6400 (10 μg of outer membrane protein noncovalently linked to capsular B polysaccharide) with the standard dose of NAGO or alum. After 28 days, all mice were boosted with the same dose of vaccine plus alum. Responses in terms of mean weight of polysaccharide-specific antibody per milliliter of serum were as follows: NAGO, 120 μg; NAGO given 1 hour before vaccine, 90 μg; GO, 72 μg; alum, 20 μg; no adjuvant <20 μg; NAGO without vaccine, <10 μg. Kinetic studies in vitro have shown that a substantial generation of Schiff base–forming ligands by NAGO occurs during the first hour and that these persist for at least 24 hours (*10*). Processing of meningococcal antigens takes longer (3 to 5 hours), but T cell determinants persist at the surface of APC for longer than 24 hours. No marked reduction in efficacy should occur when giving NAGO subcutaneously 1 hour before the antigen if direct NAGO-Ag interactions are unimportant, and this is what we found.

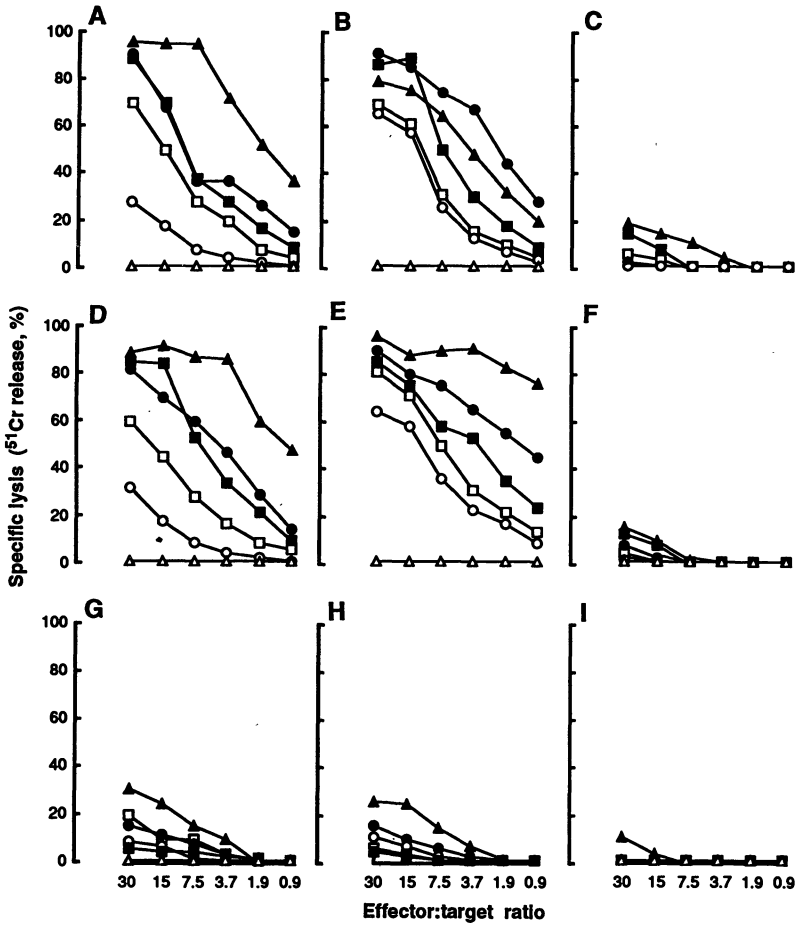

Fig. 3. Immunization with short synthetic peptide to generate CTL responses against influenza virus–infected target cells. NAGO (●); FCA (■); saponin (□); alum (○); NAGO without synthetic peptide (△); response generated by live-virus infection (▲). BALB/c mice received 100 μg subcutaneously of a hybrid peptide corresponding to CTL (amino acids 147–160) and T_H cell (amino acids 216–229) epitopes of A/PR8 influenza nucleoprotein in this strain, with the standard optimal dose of adjuvant. Another group were infected intranasally with 0.2 hemagglutinating units (HAU) of live A/PR8 virus. After 3 weeks mice were boosted by the same protocol except that FCA-primed mice received FIA. Three weeks later spleen cells were prepared and restimulated for 5 days with (**A, D,** and **G**) virus-infected syngeneic spleen cells (400 HAU per 2 × 10^7 cells), (**B, E,** and **H**) hybrid CTL-helper peptide (10 μg/ml), or (**C, F,** and **I**) serum supplemented medium only. Cells were then washed and titrated in the specific cytotoxicity assay. Target cells were P815 ($H2^d$) tumor cells labeled with $Na^{51}CrO_4$. Assays were performed on (A, B, and C) virus-infected cells (400 HAU per 2 × 10^6 P815 cells); (D, E, and F) peptide-treated cells (hybrid peptide at 10 μg/ml); and (G, H, and I) cells exposed to serum-free medium only. Cytoxicity was determined after 6 hours at 37°C by measuring released ^{51}Cr.

NAGO was generally more effective than FCA and saponin in priming T cells, but this was not fully reflected in antibody responses, where NAGO was at best comparable to the two other adjuvants. This result suggested that with NAGO as adjuvant a substantial proportion of the expanded T cell population might provide help for cytotoxic T lymphocyte (CTL) and other T cell effector mechanisms and T cell memory. The difficulty in inducing CTL with nonliving subunit vaccines has been of great concern, particularly in antiviral prophylaxis, where CTL responses are likely to be important. It is, however, possible to prime for CTL responses against influenza A–infected cells with short synthetic peptides from NP that have been identified as dominant CTL epitopes and FCA as adjuvant (*15*). When BALB/c mice were primed and boosted with a hybrid peptide that contained both helper and CTL sequences for this strain (*11, 16*), NAGO was effective as an adjuvant, comparable to FCA and saponin in priming for CTL, or even surpassing these when in vitro boosting was with peptide (Fig. 3). Moreover, responses were directed at both peptide-treated and virally infected targets. In all cases, CTL priming by peptide was compared with that induced by intranasal live-virus infection. The effect of live-virus infection was entirely reproduced in mice primed with NAGO plus peptide and restimulated in vitro with peptide before assay on virus-infected targets. Cytotoxicity was MHC class I–restricted and was inhibited by anti-CD8 but not anti-CD4 reagents. The corresponding proliferative responses were directed largely at the helper determinant (*17*).

Neither NAGO nor alum produced any trace of macroscopic lesions. Detailed histopathological evaluation in BALB/c and B10S mice showed that s.c. injection with NAGO induced a slightly lower incidence of subcutis inflammation than injection with alum, although the characteristics of the inflammatory responses for both adjuvants were similar. Differential counts of absolute numbers of subcutis neutrophils, basophils, eosinophils, macrophages, and lymphocytes in 0.2-mm^2 surrounding injection sites at 1, 3, and 6 weeks (two mice per strain) were used to establish standardized grades of inflammatory response. All reactions were graded from minimal to slight. Administration of NAGO alone subcutaneously did not lead to any increase in s.c. or lymph node lymphocyte numbers. NAGO

dosage is important because an increase in the dose limits the adjuvant effect (*18*). The amounts of NAGO that produced optimal adjuvant effects (~5 μg of GO, <50 ng of NA) are likely to be substantially less than natural exposure to ubiquitous microbial enzymes. Antibodies reacting with NA and GO were detectable in normal mouse serum. Anti-NA titers were unchanged after single NAGO use, whereas anti-GO titers were increased fivefold.

Because galactose oxidation does not compete in the conventional adjuvant pathways, it might be used in combination with conventional adjuvants and vehicles. It was not compatible with alum but showed good synergy with muramyl dipeptide (*19*) in mice (*20*). On its own, galactose oxidation was particularly potent in inducing T_H cell priming and T cell cytotoxicity and seems well suited to prophylactic applications where such responses are important (*15, 21–28*). Such use depends, of course, on the sustained absence of adverse reactions, and in this respect the absence of adverse reactions in mice looks promising.

REFERENCES AND NOTES

1. A. T. Glenny, G. C. G. Pope, H. Waddington, U. Wallace, *Chem. Ind.*, p. 415 (15 June 1926).
2. G. Gregoriadis, A. C. Allison, G. Poste, Eds., *Immunological Adjuvants and Vaccines* (Plenum, New York, 1989); M. K. Hart *et al.*, *J. Immunol.* **145**, 2677 (1990).
3. C. K. Stover *et al.*, *Nature* **351**, 456 (1991).
4. R. H. Schwartz, *Annu. Rev. Immunol.* **3**, 237 (1985); S. Buus, A. Sette, H. M. Grey, *Immunol. Rev.* **98**, 115 (1987).
5. T. A. Springer, *Nature* **345**, 426 (1990).
6. J. Rhodes, *J. Immunol.* **143**, 1482 (1989); X.-M. Gao and J. Rhodes, *ibid.* **144**, 2883 (1990); J. Rhodes, *ibid.* **145**, 463 (1990).
7. A. Novogrodsky and E. Katchalski, *Proc. Natl. Acad. Sci. U.S.A.* **70**, 1824 (1973).
8. Neuraminidase (E.C. 3.2.1.18) was from *Vibrio cholerae* (25 U per microgram of protein, BDH Poole, Dorset, United Kingdom). Galactose oxidase (E.C. 1.1.3.9) was from *Dactylium dendroides* (800 U per milligram of protein, Sigma). Standard adjuvant doses were as follows: NAGO: 1 U of NA plus 5 U of GO in 100 μl of phosphate-buffered saline (PBS) containing Ag (mixed immediately before injection); FCA (Difco): 50 μl of Ag solution emulsified in 50 μl of FCA; saponin (Quil A, Superfos, Denmark): 50 μg in 100 μl of PBS containing Ag; alum (Wellcome, Beckenham, United Kingdom): 100 μg in 100 μl of PBS containing Ag. Heat inactivation of NAGO completely abrogated the adjuvant effect. Excess D-galactose was inhibitory. GO responses were 50 to 70% of NAGO responses.
9. L. A. Lasky *et al.*, *Science* **233**, 209 (1986).
10. B. Zheng and J. Rhodes, unpublished data.
11. X.-M. Gao, F. Y. Liew, J. P. Tite, *J. Immunol.* **143**, 3007 (1989).
12. I. G. Charles *et al.*, *Proc. Natl. Acad. Sci. U.S.A.* **86**, 3554 (1989).
13. V. F. Murphy, W. C. Rowan, M. J. Page, A. A. Holder, *Parasitology* **100**, 177 (1990).
14. M. R. Lifely *et al.*, *Vaccine* **9**, 60 (1991).
15. X.-M. Gao, B. Zheng, F. Y. Liew, S. J. Brett, J. P. Tite, *J. Immunol.* **147**, 3268 (1991).
16. P. M. Taylor, J. Davey, K. Howland, J. Rothbard, B. A. Askonas, *Immunogenetics* **26**, 267 (1987).
17. B. Zheng, S. J. Brett, J. Rhodes, unpublished data.
18. B. Zheng and J. Rhodes, unpublished data.
19. L. Chedid, F. Audibert, P. Lefrancier, J. Choay, E. Lederer, *Proc. Natl. Acad. Sci. U.S.A.* **73**, 2472 (1976).
20. B. Zheng and J. Rhodes, unpublished data.
21. G. L. Ada, *Lancet* **335**, 523 (1990).
22. Y.-L. Lin and B. A. Askonas, *J. Exp. Med.* **154**, 225 (1981).
23. K.-L. Yap, G. L. Ada, I. F. C. McKenzie, *Nature* **273**, 238 (1978).
24. R. M. Ruprecht *et al.*, *Proc. Natl. Acad. Sci. U.S.A.* **87**, 5558 (1990).
25. J. H. L. Playfair, J. M. Blackwell, H. R. P. Miller, *Lancet* **335**, 1263 (1990).
26. G. C. Schild and P. D. Minor, *ibid.*, p. 1081 (1990).
27. W. C. Koff and A. S. Fauci, *AIDS* **3** (suppl. 1), S125 (1989).
28. K. S. Furukawa, K. Furukawa, F. X. Real, L. J. Old, K. O. Lloyd, *J. Exp. Med.* **169**, 583 (1989).

29. We are grateful to R. Bomford for HIV gp120. We thank M. Lockyear for PMMSA and M. Roberts for P69. We thank B. Pearce and J. Esdaile for technical assistance, and M. Stapleton for performing an enzyme-linked immunosorbent assay (ELISA) capture assay.

15 November 1991; accepted 24 March 1992

Calcium Entry Through Kainate Receptors and Resulting Potassium-Channel Blockade in Bergmann Glial Cells

T. Müller, T. Möller, T. Berger,* J. Schnitzer,† H. Kettenmann‡

Glutamate receptors, the most abundant excitatory transmitter receptors in the brain, are not restricted to neurons; they have also been detected on glial cells. Bergmann glial cells in mouse cerebellar slices revealed a kainate-type glutamate receptor with a sigmoid current-to-voltage relation, as demonstrated with the patch-clamp technique. Calcium was imaged with fura-2, and a kainate-induced increase in intracellular calcium concentration was observed, which was blocked by the non–*N*-methyl-D-aspartate (NMDA) glutamate receptor antagonist 6-cyano-7-nitroquinoxaline-2,3-dione (CNQX) and by low concentrations of external calcium, indicating that there was an influx of calcium through the kainate receptor itself. The entry of calcium led to a marked reduction in the resting (passive) potassium conductance of the cell. Purkinje cells, which have glutamatergic synapses, are closely associated with Bergmann glial cells and therefore may provide a functionally important stimulus.

During the development of the cerebellum, Bergmann glial cells provide the guiding structures for the migrating granule cells (*1*). In contrast, little is known about their function in the adult animal despite the fact that their complex architecture and intimate contacts with the Purkinje cells suggest an interaction between these two cell types. Recent studies have challenged the view of the glial cells as electrically passive elements in the brain by demonstrating the presence of many transmitter receptors, including those for glutamate (*2*). In situ hybridization studies indicate the expression of kainate-binding proteins on Bergmann glial cells (*3*). Although the subunits of the α-amino-3-hydroxy-5-methyl-4-isoxazolepropionate (AMPA)–kainate receptor channel GluR-A and GluR-D are expressed in these cells, the ubiquitous GluR-B subunit was not found (*4*). Recombinant GluR-A and GluR-D receptors exhibit a behavior distinct from other kainate receptors; namely, they have a doubly rectifying current-voltage (*I-V*) relation and high Ca^{2+} permeability (*4*).

We have used isolated slices of the mouse cerebellum to analyze membrane properties of Bergmann glial cells in situ with the patch-clamp technique (*5*) and with a fura-2–based Ca^{2+} imaging system (*6*). The Bergmann glial cell somata were recognized by their location in the Purkinje cell layer and by their small diameter (5 to 10 μm). Filling the cells with the fluorescent dyes Lucifer yellow (*7*) or fura-2 revealed the typical morphology of Bergmann glial cells: two to six processes extended through the molecular layer and terminated at the pia with the formation of glial end feet (Fig. 1, A and B). Eleven of the cells injected with Lucifer yellow were positively stained for glial fibrillary acidic protein, identifying them as astrocyte-like cells (Fig. 1C) (*8*).

Patch-clamp recordings demonstrated that the membrane was characterized by a large K^+ conductance with no sign of voltage- or time-dependent gating (Fig. 1D). Currents were observed with depolarizing and hyperpolarizing voltage steps, and the

T. Müller, T. Möller, T. Berger, H. Kettenmann, Department of Neurobiology, University of Heidelberg, Im Neuenheimer Feld 345, W-6900 Heidelberg, Germany.
J. Schnitzer, Max Planck Institute for Brain Research, Deutschordenstrasse 46, W-6000 Frankfurt, Germany.

*Present address: Institute for Anatomy, Albertstrasse 17, W-7800 Freiburg, Germany.
†Present address: Center for Molecular Medicine, Robert-Rössle-Strasse 10, O-1115 Berlin-Buch, Germany.
‡To whom correspondence should be addressed.